Edge Rotation from Momentum Transport by Neutrals

JT Omotani[1], SL Newton[1,2], I Pusztai[1] and T Fülöp[1]

[1]Department of Physics, Chalmers University of Technology, 41296 Gothenburg, Sweden
[2]CCFE, Culham Science Centre, Abingdon, Oxon, OX14 3DB, UK

Rotation and neutrals

- Rotation stabilizes resistive wall mode, flow shear suppresses turbulence in pedestal
- Intrinsic rotation important for ITER, DEMO as NBI torque weaker in larger devices
- Neutrals important for edge momentum transport due to high cross-field mobility
  – can generate intrinsic rotation in the edge
- We model effect of charge-exchange dominated neutrals coupled to neoclassical ions

Neutrals model

- Steady state radial current vanishes, small neoclassical ion viscosity, no external torque
  – constraint on neutral viscosity $\boldsymbol{\pi}_\mathrm{n}$

$$0 = j_r = \sum_a \langle e_a \boldsymbol{\Gamma}_a \cdot \nabla\psi \rangle \approx \left\langle \nabla \cdot \left(R\hat{\boldsymbol{\zeta}} \cdot \boldsymbol{\pi}_\mathrm{n} \right) \right\rangle \;\Rightarrow\; \left\langle R\hat{\boldsymbol{\zeta}} \cdot \boldsymbol{\pi}_\mathrm{n} \cdot \nabla\psi \right\rangle = 0$$

- Charge-exchange dominated neutrals, short mean-free-path expansion

$$\boldsymbol{v} \cdot \nabla f_\mathrm{n} = \frac{1}{\tau_\mathrm{CX}} \left(\frac{n_\mathrm{n}}{n_\mathrm{i}} f_\mathrm{i} - f_\mathrm{n} \right) \;\Rightarrow\; f_\mathrm{n}^{(0)} = \frac{n_\mathrm{n}}{n_\mathrm{i}} f_\mathrm{i};\; f_\mathrm{n}^{(1)} = -\tau_\mathrm{CX} \boldsymbol{v} \cdot \nabla f_\mathrm{n}^{(0)} = -\tau_\mathrm{CX} \boldsymbol{v} \cdot \nabla \left(\frac{n_\mathrm{n}}{n_\mathrm{i}} f_\mathrm{i} \right)$$

- Accounting for gyroradius correction, bulk ion distribution function

$$f_\mathrm{i}(\boldsymbol{r}) \approx f_{\mathrm{i,gc0}}(\boldsymbol{r}) - \frac{e\Phi_1}{T_\mathrm{i}} f_{\mathrm{i,gc0}}(\boldsymbol{r}) - \boldsymbol{\rho} \cdot \nabla f_{\mathrm{i,gc0}}(\boldsymbol{r}) + g_\mathrm{i}(\boldsymbol{r})$$

- Assume $n_\mathrm{n}/n_\mathrm{i}$ small enough that neutrals do not affect f_i directly, gives

$$R\hat{\boldsymbol{\zeta}} \cdot \boldsymbol{\pi}_\mathrm{n} \cdot \nabla\psi = \frac{\tau_\mathrm{CX} R^4 B_\mathrm{p}^4 T_\mathrm{i}^2}{eB^2} \frac{dn_\mathrm{n}}{d\psi} \left(\frac{d\ln p_\mathrm{i}}{d\psi} + \frac{e}{T_\mathrm{i}} \frac{d\Phi_0}{d\psi} + \frac{d\ln T_\mathrm{i}}{d\psi} \right) - \frac{\tau_\mathrm{CX} R^2 B_\mathrm{p}^2 I m_\mathrm{i}}{2Bn_\mathrm{i}} \frac{dn_\mathrm{n}}{d\psi} \int d^3v\, v_\parallel v_\perp^2 g_\mathrm{i}$$

- Large compared to neoclassical $\boldsymbol{\pi}_\mathrm{i}$ due to strong anisotropy in gyroangle of f_n
- Useful expressions for interpretation:
  – toroidal flow and heat flux take general form [1]

$$V_{\mathrm{i}\zeta} = -R \left(\frac{d\Phi_0}{d\psi} + \frac{1}{en_\mathrm{i}} \frac{dp_\mathrm{i}}{d\psi} \right) - \frac{kI^2}{Re\left\langle B^2 \right\rangle} \frac{dT_\mathrm{i}}{d\psi};\; q_{\mathrm{i}\zeta} = -\frac{5Rp_\mathrm{i}}{2e} \frac{dT_\mathrm{i}}{d\psi} + \frac{5lI^2 p_\mathrm{i}}{2Re\left\langle B^2 \right\rangle} \frac{dT_\mathrm{i}}{d\psi}$$

  – momentum flux is balance between friction and heat friction

$$\left(R\hat{\boldsymbol{\zeta}} \cdot \boldsymbol{\pi}_\mathrm{n} \cdot \nabla\psi \right) \approx -\tau_\mathrm{CX} R^3 B_\mathrm{p}^2 T_\mathrm{i} \frac{dn_\mathrm{n}}{d\psi} \left(V_{\mathrm{i}\zeta} + \frac{2}{5p_\mathrm{i}} q_{\mathrm{i}\zeta} \right) + \frac{\tau_\mathrm{CX} R^2 B_\mathrm{p}^2 I m_\mathrm{i}}{5Bn_\mathrm{i}} \frac{dn_\mathrm{n}}{d\psi} \int d^3v\, v^3 P_3(\xi) g_\mathrm{i}$$

Simulation setup

- Ion distribution function from PERFECT [2]
- Iterate on $\frac{d\Phi_0}{d\psi}$ to satisfy steady-state constraint
- Model ITER-like equilibrium [3]
  – baseline parameters: $\epsilon = 0.32$, $\kappa = 1.7$, $\delta = 0.33$, $R_\mathrm{X} = (1 - 1.1\delta\epsilon)R_0$, $Z_\mathrm{X} = -1.1\kappa\epsilon R_0$, $I_\mathrm{P} = 15\ \mathrm{MA}$, $\beta_\mathrm{t} = 0.05$, $R_0 = 6.2\ \mathrm{m}$, $B_0 = 5.3\ \mathrm{T}$
- Nominal plasma parameters $T_\mathrm{i} = 300\ \mathrm{eV}$, $n_\mathrm{i} = 10^{20}\ \mathrm{m}^{-3}$ in baseline equilibrium give collisionality $\frac{\nu_\mathrm{ii} L_\parallel}{v_\mathrm{T}} \approx 1.26$. Collisionality varied in scans by changing density
- Drive term is $\frac{d\ln T_\mathrm{i}}{d\psi}$, set to value corresponding to $\frac{d\ln T_\mathrm{i}}{dr} = -\frac{1}{L_{T\mathrm{i}}}$ for $L_{T\mathrm{i}} = 10\ \mathrm{cm}^{-1}$ at outboard midplane of baseline equilibrium
- Density gradient only gives offset to $\frac{d\Phi_0}{d\psi}$, so set $\frac{dn_\mathrm{i}}{d\psi} = 0$ here
- Solve on $\psi_\mathrm{N} = 0.95$ flux surface
- Poloidally localized neutrals, represented by delta-function

Analytical comparison

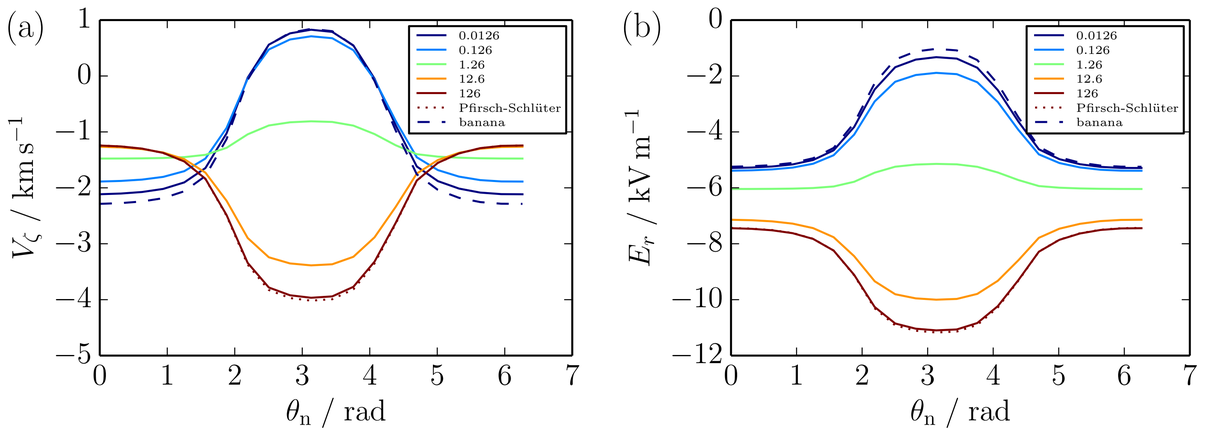

Figure 1: (a) Toroidal rotation and (b) radial electric field against poloidal location of neutrals. Simulation results (solid), legend gives collisionality. Pfirsch-Schlüter (red dotted) and banana (blue dashed) analytical limits. $\theta_\mathrm{n} = 0$ is outboard midplane

- Analytical limits for E_r and $V_{\mathrm{i}\zeta}$ calculated in [4]
- Good agreement with simulation results found at both high and low collisionality

[1] P Helander and DJ Sigmar. *Collisional transport in magnetized plasmas*. 2002.
[2] M Landreman, FI Parra, PJ Catto, DR Ernst, and I Pusztai. *Plasma Phys. Controlled Fusion*, 56(4):045005, 2014.
[3] AJ Cerfon and JP Freidberg. *Phys. Plasmas*, 17(3):032502, 2010.
[4] P Helander, T Fülöp, and PJ Catto. *Phys. Plasmas*, 10(11):4396, 2003.
[5] YB Kim, PH Diamond, and RJ Groebner. *Phys. Fluids B*, 3(8):2050, 1991.
[6] PJ Catto and AN Simakov. *Phys. Plasmas*, 13(5):052507, 2006.

Neutral Location

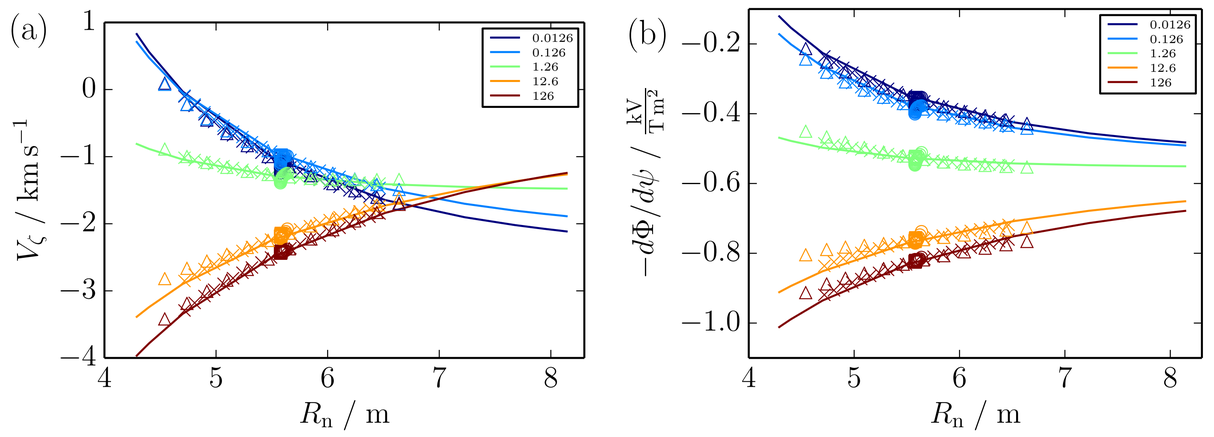

Figure 2: Response of (a) toroidal rotation and (b) radial electric field to major radius of localized neutrals for scan in poloidal angle (solid line), and R_X (×), Z_X (□), κ (○) and δ (△) with neutrals localized at X-point. Legend gives collisionality

- Poloidal scan represents different fuelling locations in baseline geometry
- Geometry scans have neutrals fixed at X-point, representing divertor recycling or PFR fuelling
- Controlling parameters: major radius where neutrals localized, R_n, and plasma collisionality
- All shaping parameters except ϵ affect $V_{\mathrm{i}\zeta}$ and $-d\Phi/d\psi$ only through changing R_n

Inverse aspect ratio

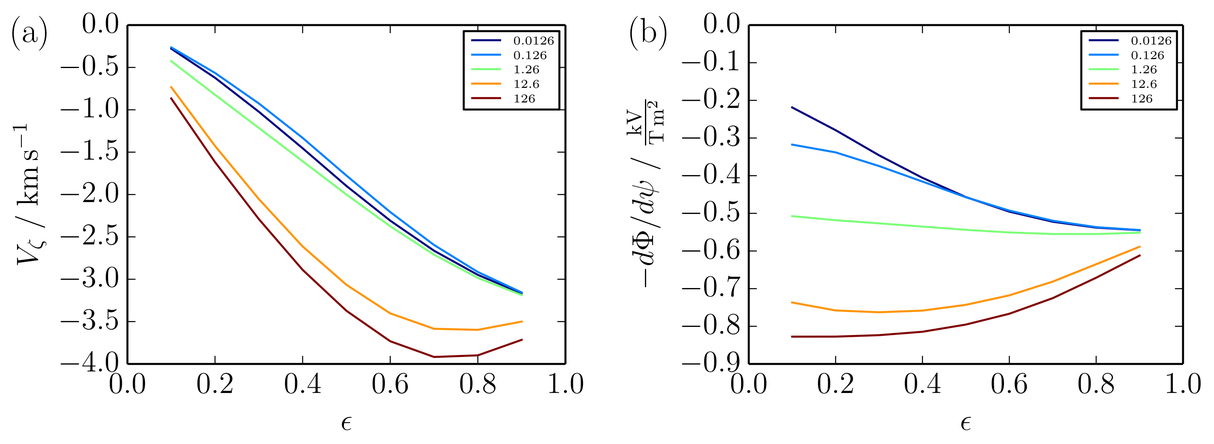

Figure 3: Response of (a) toroidal rotation and (b) radial electric field to ϵ. Legend gives collisionality

- ϵ has effect on $V_{\mathrm{i}\zeta}$ and E_r beyond R_n, unlike higher order shaping parameters
- $\epsilon \to 1$ limit: poloidal flow suppressed by mirror force inboard
  $\Rightarrow -\frac{d\Phi_0}{d\psi} \to \frac{2}{e}\frac{dT_\mathrm{i}}{d\psi} \approx -0.547\ \mathrm{kV\,T^{-1}\,m^{-2}}$, $V_{\mathrm{i}\zeta} \to \frac{R}{e}\frac{dT_\mathrm{i}}{d\psi} \approx -3.39\ \mathrm{km\,s^{-1}}$
- Large aspect ratio, $\epsilon \to 0$: $B \to I/R$, $l \to 1$. Toroidal heat flux vanishes $q_{\mathrm{i}\zeta} \to 0$ so no intrinsic momentum transport, toroidal rotation vanishes $V_{\mathrm{i}\zeta} \to 0$

Impurity rotation

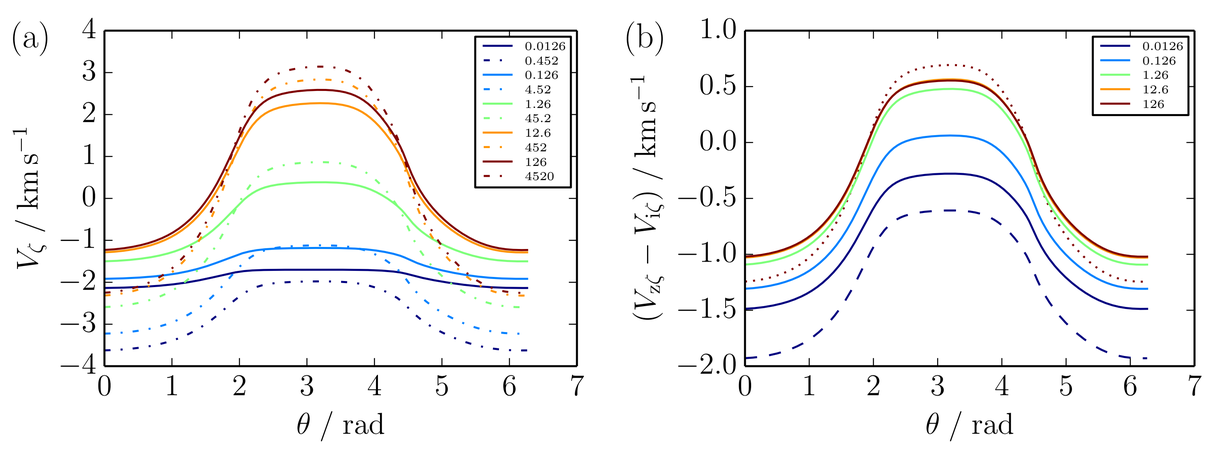

Figure 4: Poloidal variation of (a) toroidal rotation for bulk deuterium (solid) and trace, fully ionized carbon (dash-dotted) with neutrals at outboard midplane and (b) velocity difference between carbon and bulk (solid) compared to analytical calculation for collisional impurity with collisional (dotted) or collisionless (dashed) bulk. Legend gives collisionality. $\theta = 0$ is outboard midplane. $n_\mathrm{Z}/n_\mathrm{i} \approx 0.018$

- Calculate impurity rotation to compare to CXRS measurements
- Trace impurity: impurity-neutral coupling neglected
- Bulk ion and impurity rotation differ, as expected [5]
- Analytical forms for velocity difference between impurity and ions given for collisional and mixed (collisional impurity, banana bulk) limits in [6]
  – 30% discrepancy is $\mathcal{O}(Z^{-1})$, also approximate collision operators used analytically
- $(V_{\mathrm{i}\zeta} - V_{\mathrm{Z}\zeta})$ independent of $\frac{d\Phi_0}{d\psi}$, so independent of neutral location $\Rightarrow$ (b) identical for any θ_n

Conclusions

- We calculate toroidal momentum transport through charge-exchanging neutrals
  – outputs: radial electric field, rotation velocity
- Allow arbitrary collisionality using numerical solutions for ion distribution
- Rotation of trace impurity can be calculated to assist experimental comparison
- Good agreement with analytical limits at high and low collisionality
- Control parameters R_n, bulk collisionality, ϵ
  – higher order shaping parameters affect outputs only through changing R_n

Email: omotani@chalmers.se